

## Chapter V AOPs

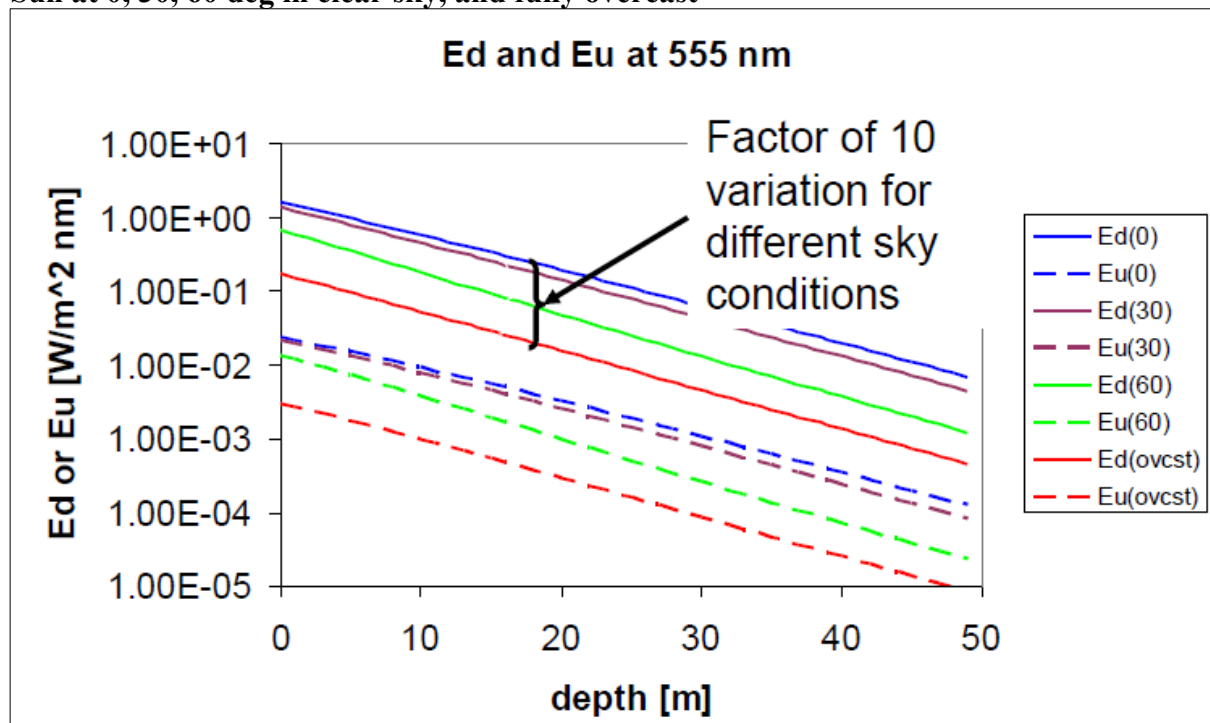
AOP = Apparent Optical Property

### 1) AOPs in marine water

It is convenient to define the environmental **properties** in a way that allows you to study their changes over time or compare them with the properties at a different study site. The same approach as for IOPs was therefore tried for light. However, since light generally decreases very quickly with depth it is not a stable parameter.

**HydroLight runs: Chl = 1.0 mg Chl/m<sup>3</sup>, etc**

**Sun at 0, 30, 60 deg in clear sky, and fully overcast**



Ed and Eu depend on L and the IOPs of the water, but they also strongly depend on the ambient conditions and are not very useful at all to characterise a water column (they are not AOPs!)

In contrast, it has been observed that light intensity generally diminishes exponentially with depth which means that the slope of the exponential is constant. In fact, the slope of the logarithm of light intensity (slopes of ln(PAR), ln(Ed), or ln(Eu)) is an optical property (unit: m<sup>-1</sup>). However, it does not only depend on the environment but on the light itself. This property is therefore not inherent but “apparent”; it is an AOP: Apparent Optical Property.

The **spectral diffuse attenuation coefficient K in m<sup>-1</sup>** (not to be confused with the attenuation coefficient c) is thus defined by the downwelling irradiance:

$$K_d(z) = \frac{-d(\ln E_d(z))}{dz} \quad \text{and also} \quad K_d(z) = \frac{-1}{E_d(z)} \frac{d(E_d(z))}{dz}$$

This diffuse attenuation coefficient is obviously wavelength dependent. It can also be defined for Eu, PAR, etc.

Be careful with the second definition above which should not be used without giving some consideration to the value of  $E_d$  in the denominator (at which depth should we choose it? If we use this approach to calculate  $K_d$  the error increases if the derivative is calculated at rather distant depths, i.e., if  $dz$  is large).

### Optical thickness

About 90% of the light that leaves the water comes from a layer of thickness  $1/K_d$ , called the “**optical thickness**” (Gordon & Mc Cluney, 1975; Gordon & Morel, 1983). In remote sensing, this thickness  $z_{opt}$  (or  $z_{pd}$  for “penetration depth”) is very important. The more phytoplankton or suspended matter there is in the water, the greater  $K_d$  and thus the smaller the optical thickness, i.e., the part of the surface layer that can be “seen” by satellites.

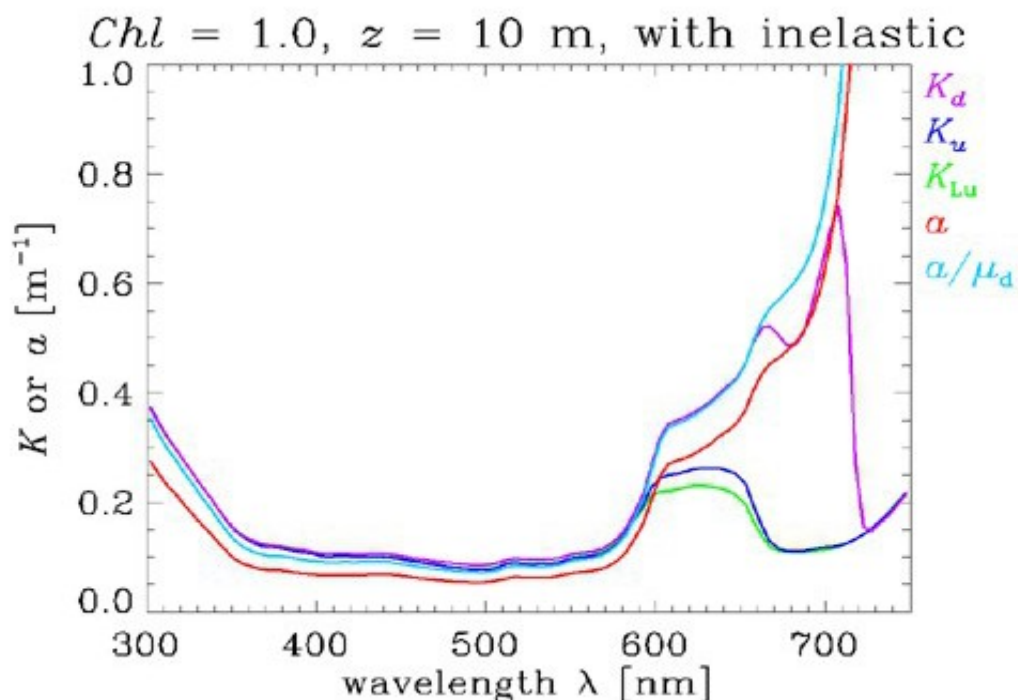
Exercise Calculate the downwelling irradiance at the bottom of this layer  $E_d(z_{opt})$  as a function of surface irradiance. State the relation between this irradiance and the irradiance at the base of the euphotic zone as well as the relation between  $z_{eu}$  and  $z_{opt}$ .

If we use  $K_{par}$  instead of  $K_d$  to calculate the optical thickness using the example from the previous figure, we can estimate that the optical thickness at each station is

Station 1  $z_{opt} = 20$  m      Station 2  $z_{opt} = 10$  m

Is this reasonable given the depth of the euphotic layer?

$K_d$  is a spectral quantity and can be estimated for a fixed chlorophyll concentration; see below.



[http://www.oceanopticsbook.info/view/overview\\_of\\_optical\\_oceanography/k\\_functions](http://www.oceanopticsbook.info/view/overview_of_optical_oceanography/k_functions)

Fig. 5.  $K$  at 10 m depth for Case 1 water with . The HydroLight run included Raman scatter by the water and chlorophyll as well as CDOM fluorescence.

$K_{par}$  is obviously not a spectral quantity and cannot be represented in this way.

In contrast,  $K_{par}$  can be represented as a function of ambient pigment concentration:

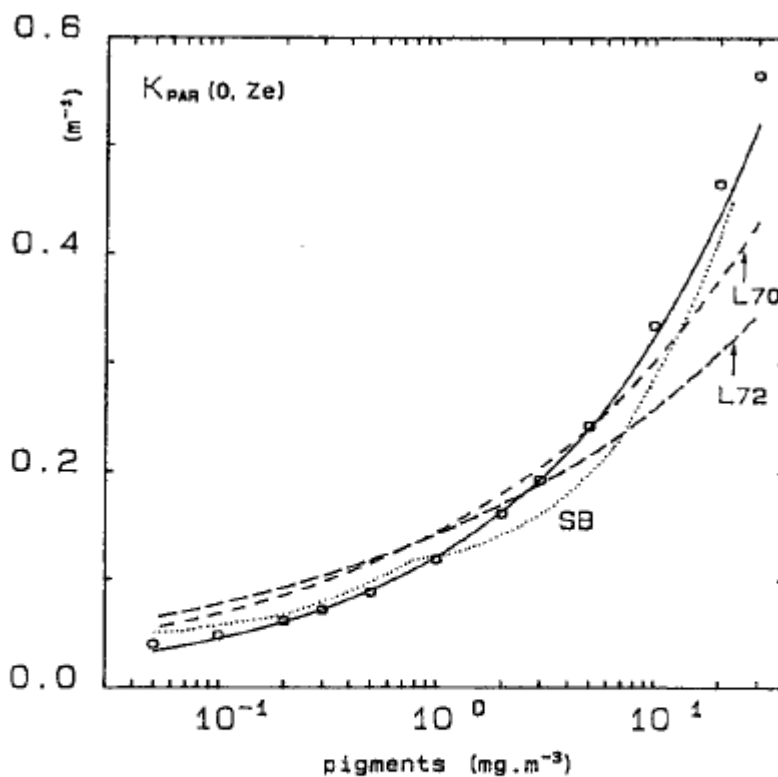
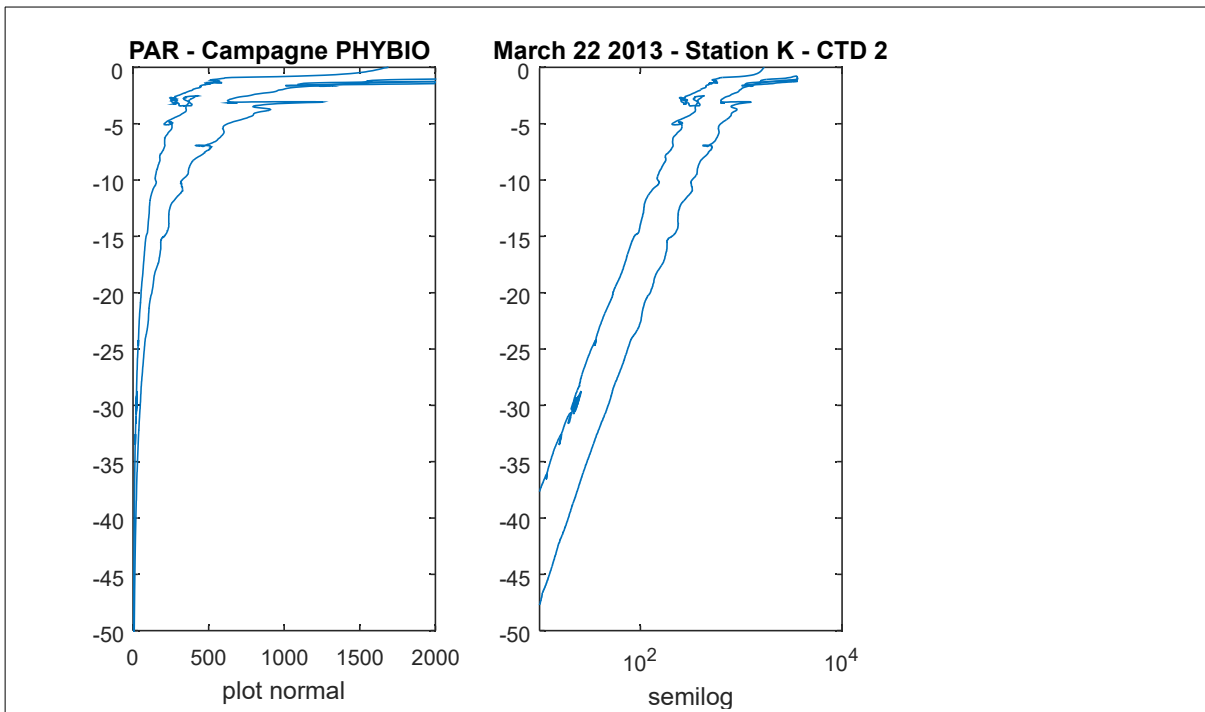


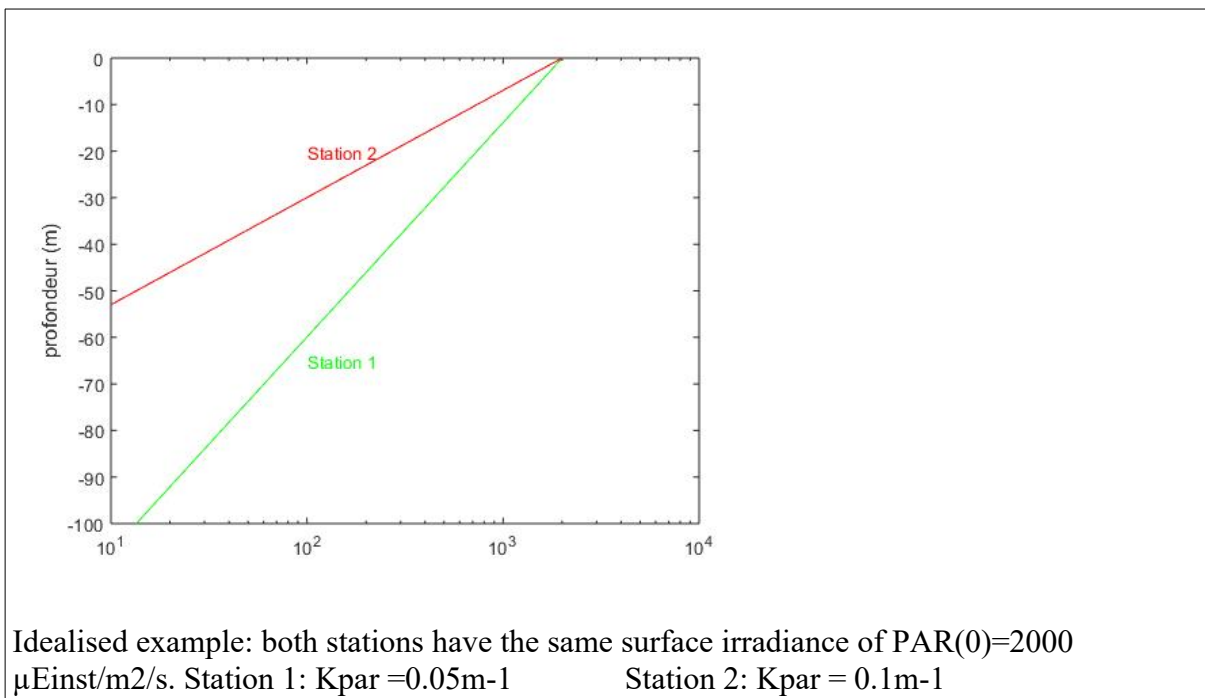
Fig. 3a. Attenuation coefficient for downwelling photosynthetically available radiation,  $\bar{K}_{\text{PAR}}$ , as a function of the mean pigment concentration within the euphotic layer; solid curve according to (5), curves labeled SB from *Smith and Baker* [1978] and L70 and L72 derived from the data of *Lorenzen* [1970, 1972]. The circles correspond to the products of the spectral model (see text and equations (11) and (4)).

Figure from Morel, A. (1988). Optical modeling of the upper ocean in relation to its biogenous matter content (Case 1 water), *Journal of Geophysical Research*, 93, 10,749-10,768.

The sunshine conditions can change while the environment remains the same. In this case, even if  $E_d$  or surface PAR are very different, the curves in the semilog plot remain parallel, i.e., they have the same slope; this means that the  $K_d$  or  $K_{\text{PAR}}$  is the same. Example with PAR below.



On the other hand, we can have the same sunshine conditions at the surface either i) in two different locations or ii) in the same location but at two different times; if the IOPs of the water column are not the same then the slopes are different as well (see following figure).



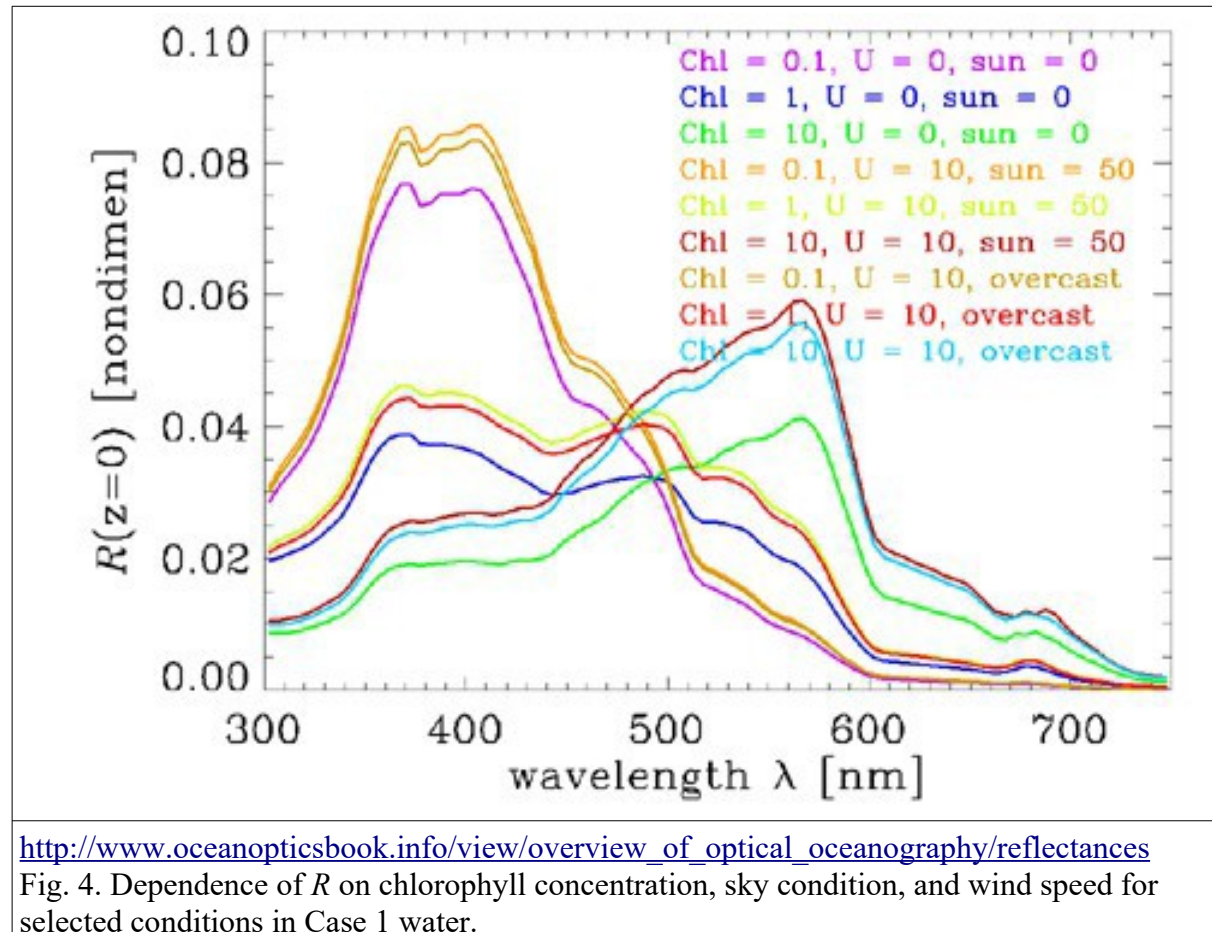
Note: it has been pointed out recently how Kpar may not be completely accurate. For example, see this excerpt from Lee Zhongping (2009) “Kpar: An optical property associated with ambiguous values. Journal of Lake Sciences”:

“As shown in various studies[12,33], treating KPAR as a depth-independent property is not consistent with the physics of light propagation through an aquatic environment; and such KPAR approach results in coarse, if not erroneous, approximation of PAR’s vertical profile. In a broader perspective, these inconsistencies indicate that depth-independent KPAR is not a robust candidate to be considered as a stand-alone product (in analogy to concentration of chlorophyll) for ocean color remote sensing. (...) Presently, KPAR can be modeled from other well-defined properties or products, such as the diffuse attenuation coefficient at 490nm [ $K_{490}$ ] [20], concentration of chlorophyll [36-37], and the inherent optical properties [19,38]. Separately, for the application of measuring water quality from observation of water color [10], instead of using the ambiguous KPAR, it is better to use water’s inherent optical properties [39-40] or photic depths [41].”

**Hence the availability of  $K_{490}$  on the CMEMS Mercator platform.**

Likewise, **reflectance**, the ratio between upwelling and downwelling irradiance, is generally fairly constant for a given water mass and is therefore defined as an AOP:

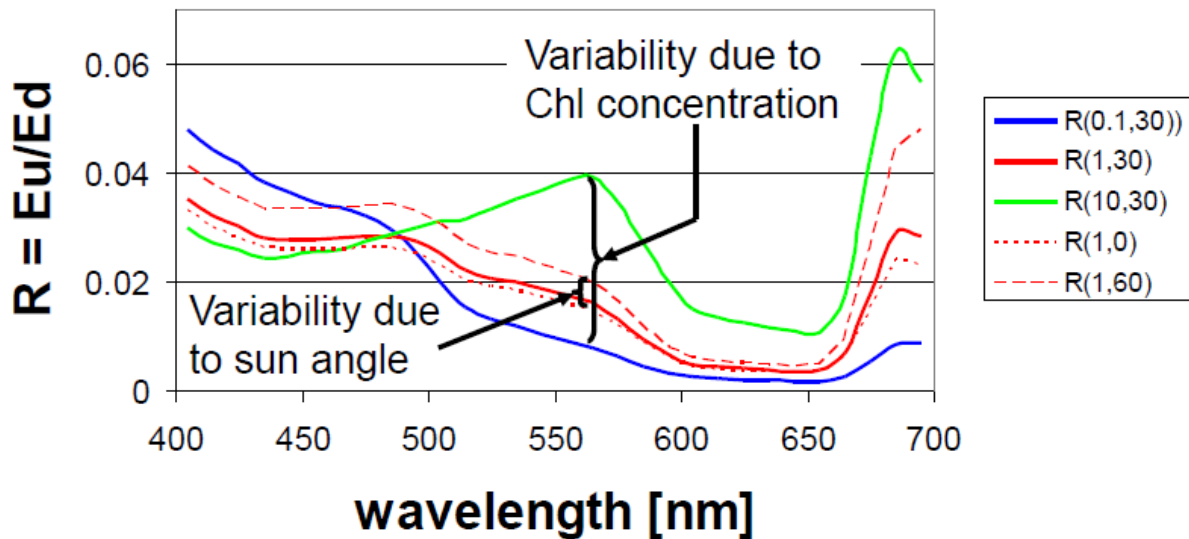
$$R = \frac{E_u}{E_d} \quad (\text{dimensionless})$$



[http://www.oceanopticsbook.info/view/overview\\_of\\_optical\\_oceanography/reflectances](http://www.oceanopticsbook.info/view/overview_of_optical_oceanography/reflectances)  
Fig. 4. Dependence of  $R$  on chlorophyll concentration, sky condition, and wind speed for selected conditions in Case 1 water.

*Ex - HydroLight runs: Chl = 0.1, 1, 10 mg Chl/m<sup>3</sup>  
Sun at 0, 30, 60 deg in clear sky*

R(Chl,sun) at 5 m



R depends to some extend on the ambient conditions but mostly on the water column's IOPs.

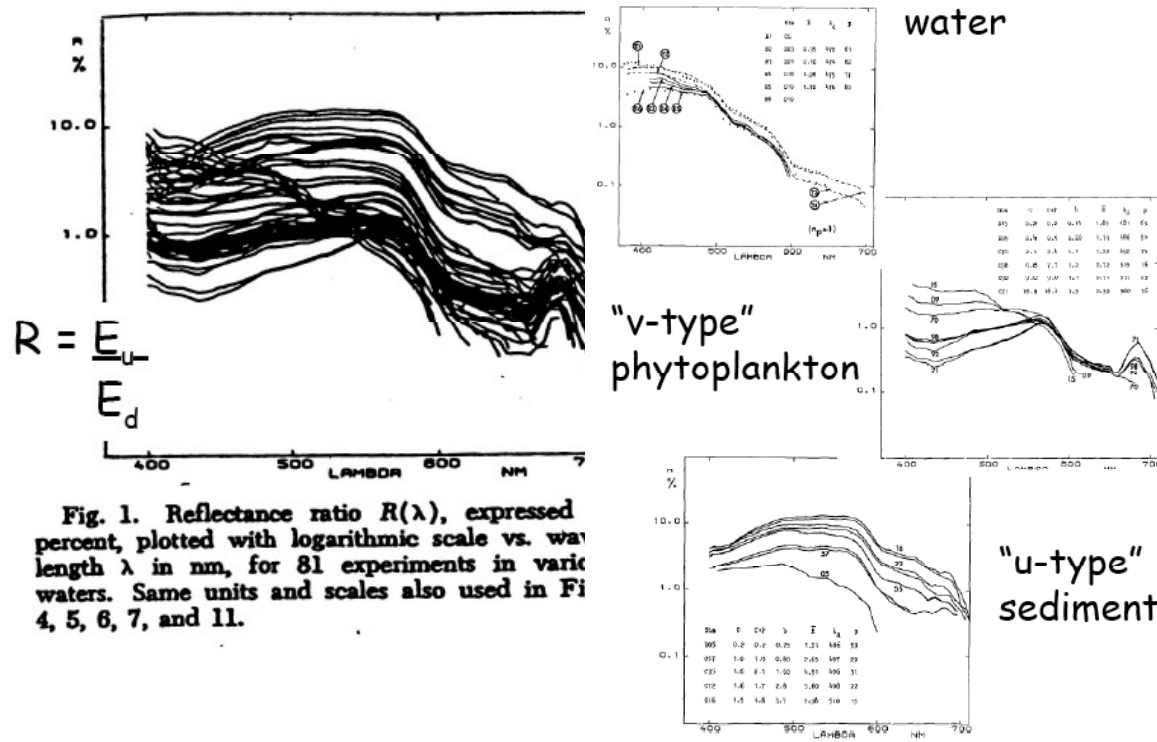
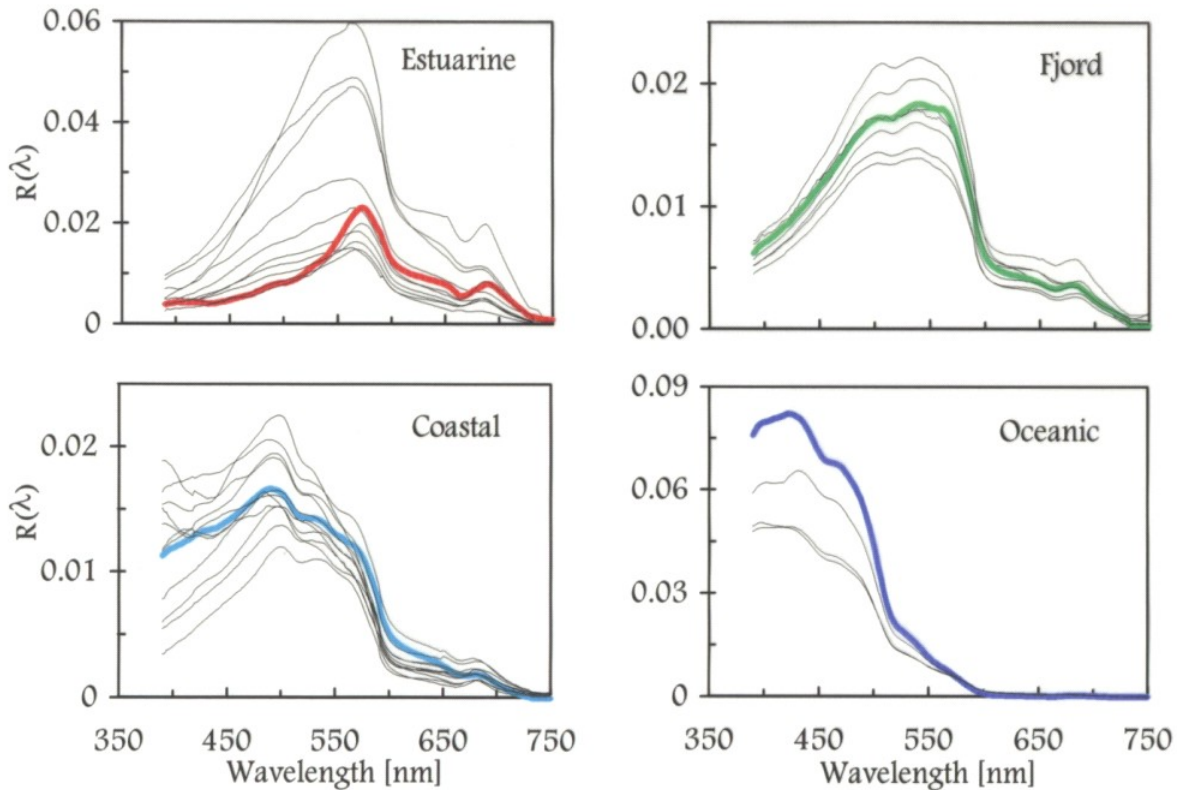


Fig. 1. Reflectance ratio  $R(\lambda)$ , expressed percent, plotted with logarithmic scale vs. wavelength  $\lambda$  in nm, for 81 experiments in various waters. Same units and scales also used in Figs. 4, 5, 6, 7, and 11.

Morel and Prieur, 1977 Analysis of variations in ocean color, Limnol Oceanogr 22, 709-722.



### Roesler and Perry 1995

Article by Roesler and Perry (1995)

The chlorophyll concentrations vary between sites:

Estuarine from 4 to 25 mg/m<sup>3</sup>

Fjord from 1.25 to 2 mg/m<sup>3</sup>

Coastal from 0.5 to 2.8 mg/m<sup>3</sup>

Oceanic from 0.07 to 0.09 mg/m<sup>3</sup>

This explains in part the shape and intensity of the spectrum (see the rest of their paper for the influence of other factors such as backscattering).

Following to advent of remote sensing, it was necessary to introduce a quantity called **“remote-sensing reflectance”** which is the ratio between the water-leaving radiance ( $L_w$ ) and the downwelling irradiance:

$$R_{rs} = \frac{L_w}{E_d} \quad (\text{unit: sr}^{-1})$$

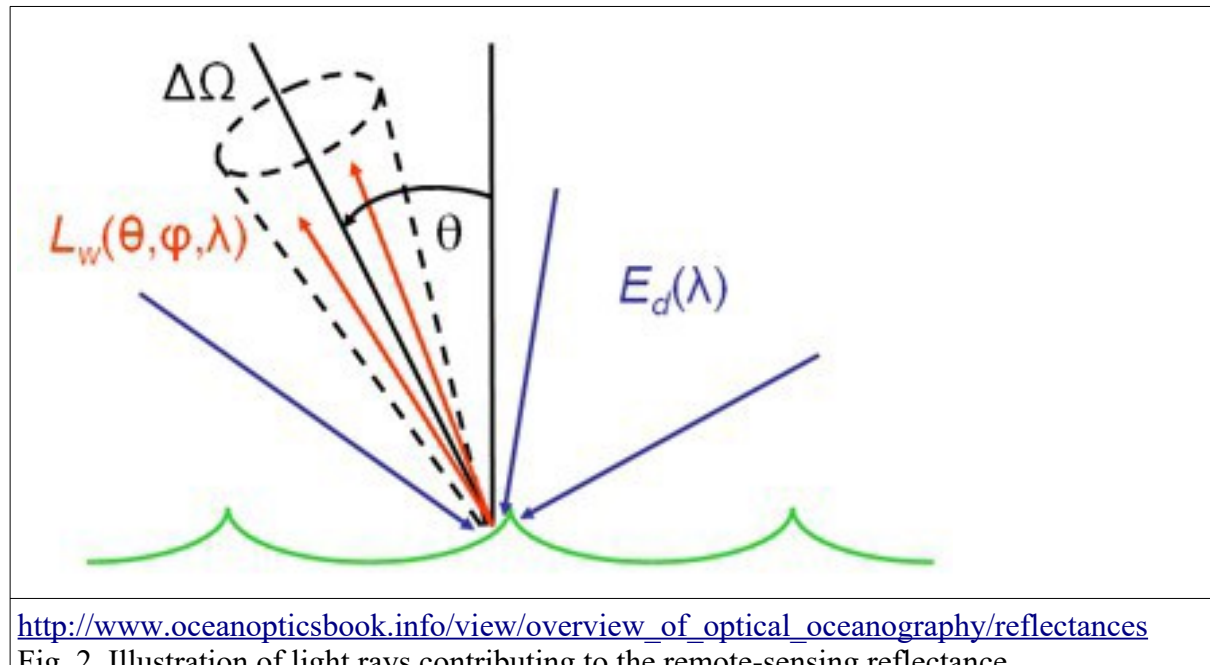
The parameter typically refers to the 0+ level, i.e., just above the sea surface.

$$R_{rs}(0^+, \theta, \varphi) = \frac{L_w(0^+, \theta, \varphi)}{E_d(0^+)}$$

Typically, when a radiometer measures the radiance ( $L_m$ ) above the water surface, it not only records the radiance leaving the water but also the light reflected at the surface. To eliminate this component, Mobley (1999) recommended to subtract the radiance from the sky,  $L_{sky}$ , multiplied by  $\rho$ , the reflectance which depends on the angle of incidence of the light from the

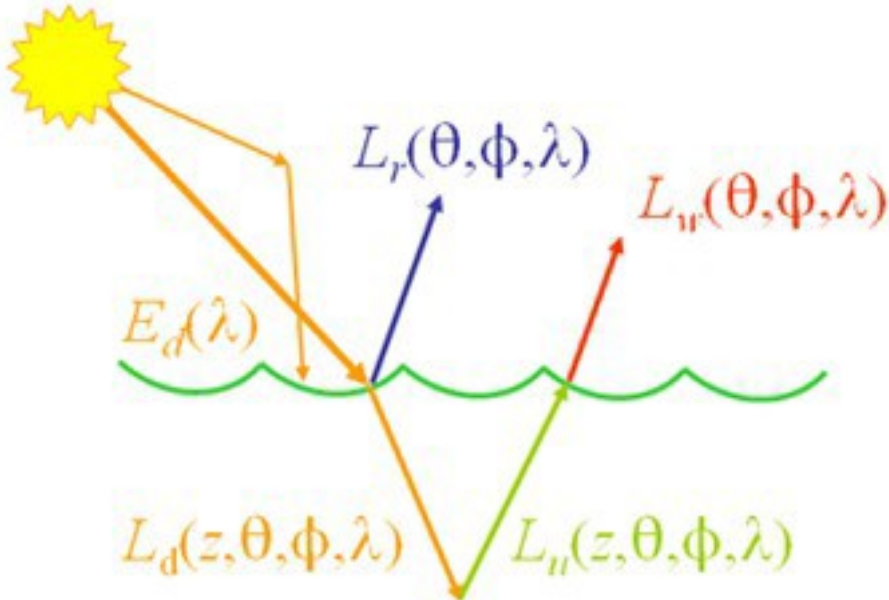
sun, the cloud cover and the sea state (presence of waves/capillary waves). The surface leaving radiance is thus  $L_w = L_m - \rho \times L_{sky}$

Hence  $R_{rs}(0^+) = (L_m - \rho \times L_{sky})/E_d$



To determine  $R_{rs}$  we thus need to measure three different quantities:  $L_m$ ,  $E_d$ , and  $L_{sky}$ . Radiance measurements are typically made at an azimuthal angle of  $135^\circ$  with respect to the sun to reduce the amount of sun glint from the surface and at a polar angle of  $45^\circ$  (following the recommendations by Mobley, 1999).  $E_d$  can either be modelled (but in this case the cloud cover is often neglected or only accounted for in a highly simplified manner) or measured using a suitable radiometer.

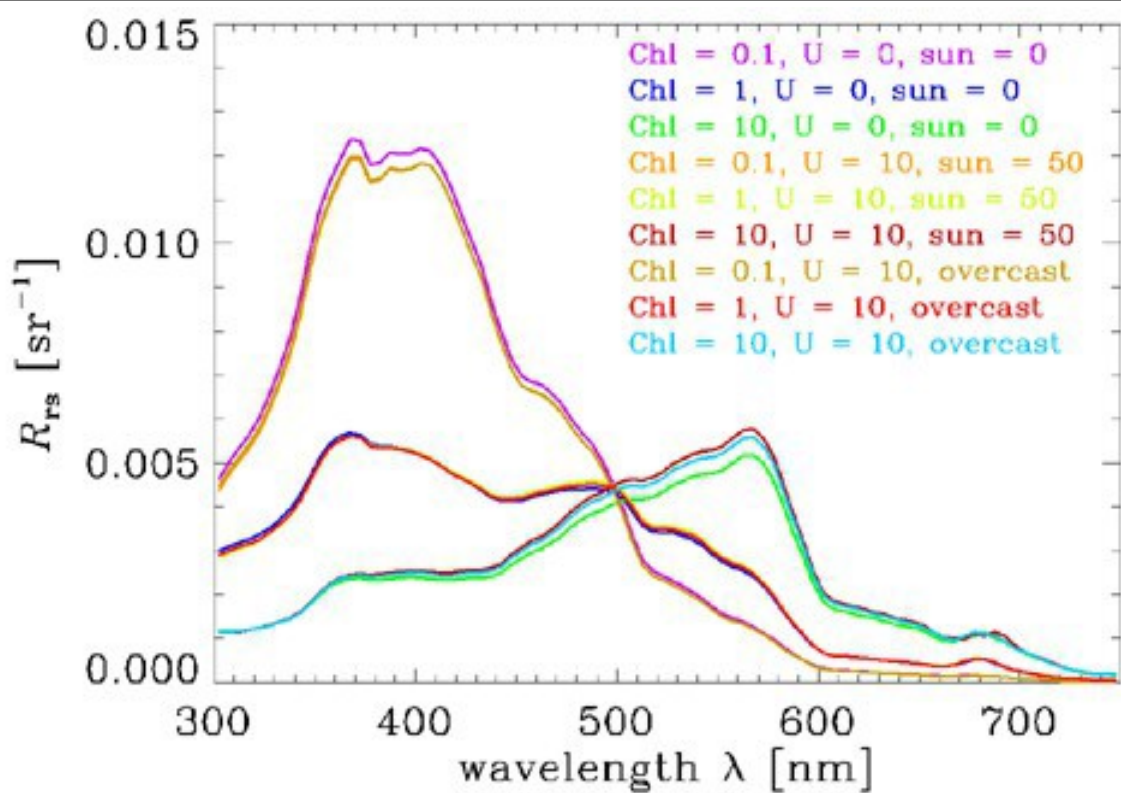
$$L_u(\text{in air}, \theta, \phi, \lambda) = L_w(\theta, \phi, \lambda) + L_r(\theta, \phi, \lambda)$$



[http://www.oceanopticsbook.info/view/overview\\_of\\_optical\\_oceanography/reflectances](http://www.oceanopticsbook.info/view/overview_of_optical_oceanography/reflectances)

Fig. 3. Illustration of light rays contributing to  $L_u$  as measured above the sea surface.

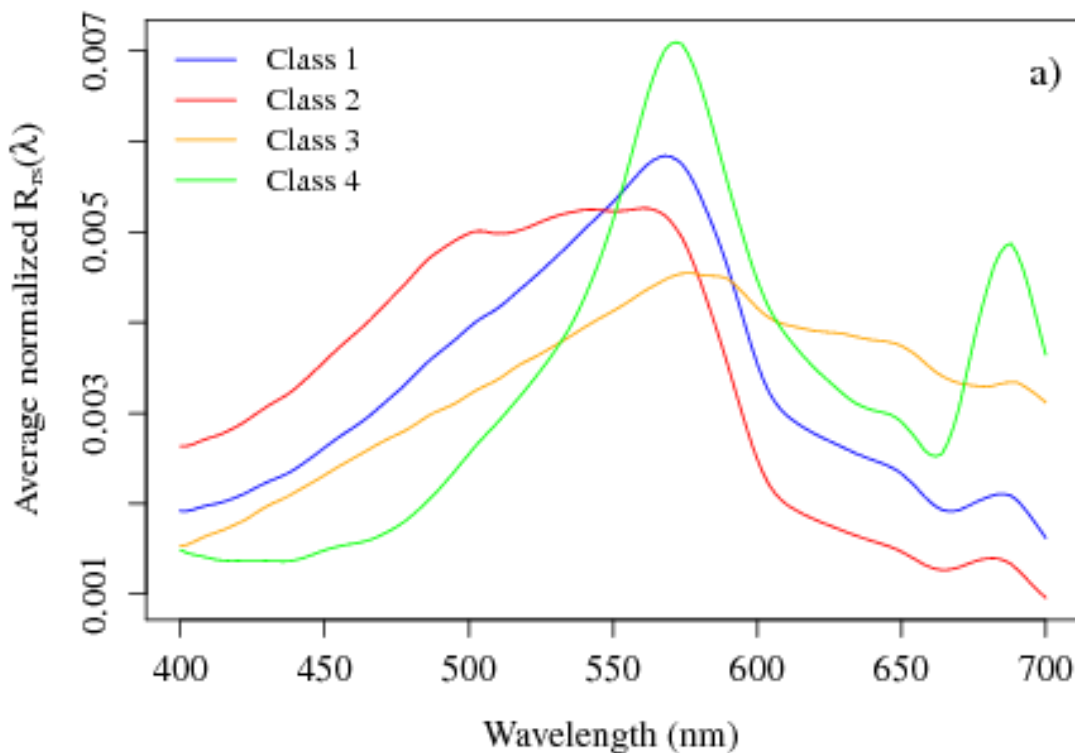
If the measurement is not made at sea level but by a satellite, then, more than 80-90% of the radiance  $L_m$  as measured by the satellite comes from the atmosphere. Oceanographic applications therefore always require an “atmospheric correction” to be applied to any measurements to obtain  $L_w$ .



[http://www.oceanopticsbook.info/view/overview\\_of\\_optical\\_oceanography/reflectances](http://www.oceanopticsbook.info/view/overview_of_optical_oceanography/reflectances)

Fig. 5. Dependence of  $R_{rs}$  on chlorophyll concentration, sky condition, and wind speed for selected conditions in Case 1 water.

We again note the three main groups of reflectance as a function of chlorophyll concentration.



Class 1: Mixed + sediments

Class 2: Mixed + phytoplankton

Class 3: +++ sediments

Class 4 : +++ phytoplankton & CDOM

normalised remote sensing reflectances (Vantrepotte et al.)

The statistical analyses by Teodoro et al. [2008] on measurements off Portugal show a positive effect of the amount of particulate matter in the water column on the reflectance at visible wavelengths.

Teodoro, A. C., Veloso-Gomes, F., & Gonçalves, H. (2008). Statistical techniques for correlating total suspended matter concentration with seawater reflectance using multispectral satellite data. *Journal of Coastal Research*, 24(sp3), 40-49.

(courtesy S. Sergi (OPB 2016-17) for the modified Teodoro figure)

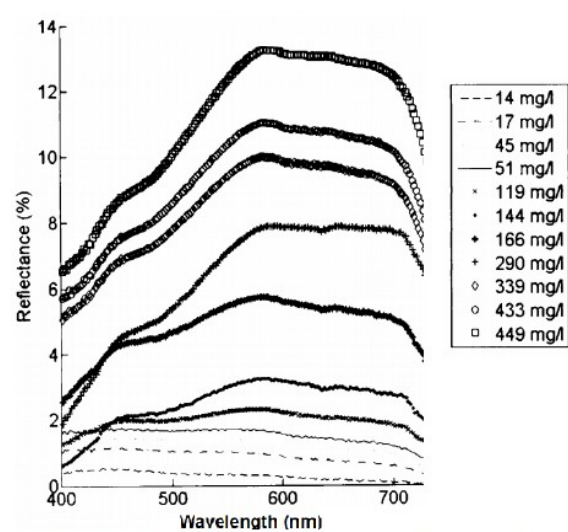


Figure 2: Relation entre la charge en matière particulaire dans la colonne d'eau et la réflectance de l'eau de mer. Modifié d'après Teodoro et al., 2008.

The mean cosine, written as  $\bar{\mu}_d$ , is the ratio between  $E_d$  (downwelling “cosine” irradiance) and  $E_{od}$  (scalar downwelling irradiance). It is a dimensionless quantity and forms part of the family of AOPs. It can also be defined in terms of  $E_u$  or in a more general fashion:

$$\bar{\mu}_d = \frac{E_d}{E_{od}} \quad ; \quad \bar{\mu}_u = \frac{E_u}{E_{ou}} \quad ; \quad \bar{\mu} = \frac{E_d - E_u}{E_o}$$

## 2) The Gordon normalisation of Kd – water classification

$K_d$  can be normalised using (Gordon, 1989a):

$$nK_d(\lambda) = \frac{Kd}{Do} \quad (\text{Gordon, 1989}) \quad \text{with } Do = fDo(\text{sun}) + (1-f) Do(\text{sky})$$

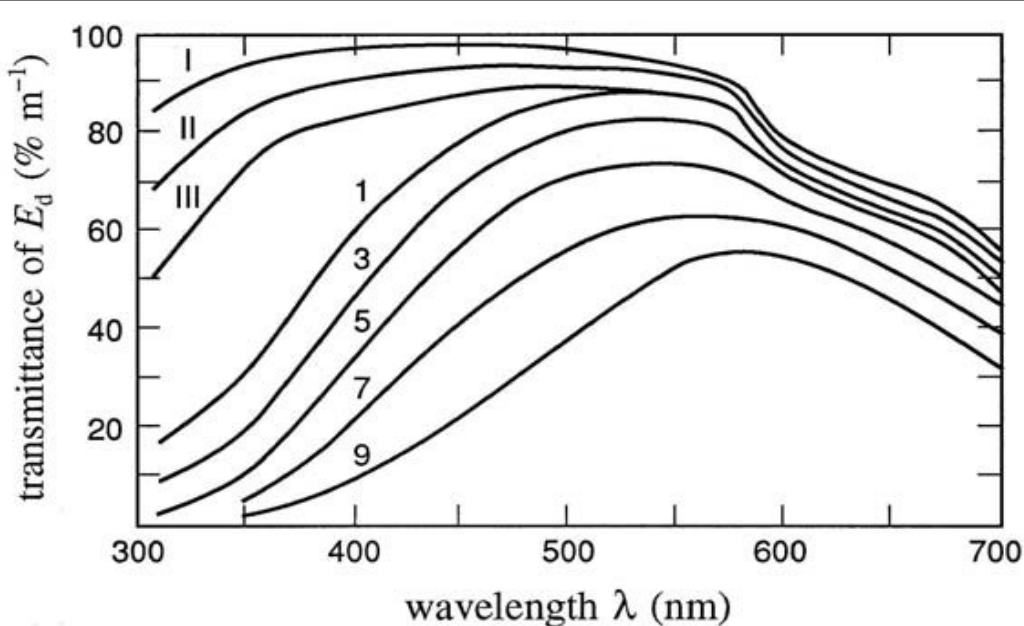
$f$  represents the fraction of direct sunlight that passes from air to the water as part of the total incident irradiance.  $Do(\text{sun}) = 1/\cos(\theta_{sw})$

$\theta_{sw}$  is the nadir angle of the transmitted ray in water with respect to the solar zenith angle in air (thus equal to  $\arcsin(\sin(\theta_s)/nw)$  with  $\theta_s$  the solar zenith angle in air and  $n_w$  the index of refraction of water).  $Do(\text{sky})$  is due to radiance from the sky.

The normalised  $K_d$  becomes an IOP as it no longer depends on the sea state or the light itself. It would correspond (if  $Do=1$ ) to a sun at the zenith shining in a black sky (no scattering), above a completely calm sea.

Otherwise,  $K_d$  is generally considered a quasi-IOP.

Moreover, the first classification of marine waters depended on  $K_d$  (Jerlov, 1976) and consisted of various categories. Offshore water were divided into Case I, IA, IB, II, and III waters while coastal areas into Case 1, 2, 3, ... 9 waters.



Percentage transmittance of downwelling irradiance,  $E_d$ , per meter of water, as a function of wavelength, for selected Jerlov water types. [reproduced from Jerlov (1976), by permission] via Mobley 1994

Morel (1988) established a link between the chlorophyll concentration and the Jerlov water classification types.

type	I	IA	IB	II	III
chl	0-0.01	0.05	0.1	0.5	1.5-2

Austin and Petzold (1986) presented a quantitative classification scheme that allowed for  $K_d$  to be directly derived from the Jerlov water type.

**Table 3.15.** Downwelling irradiance diffuse attenuation coefficients  $K_d(\lambda)$  used to define the Jerlov water types, as determined by Austin and Petzold.<sup>a</sup>  
All quantities in the body of the table have units of  $\text{m}^{-1}$ .

$\lambda$ (nm)	Jerlov water type					
	I	IA	IB	II	III	1
350	0.0510	0.0632	0.0782	0.1325	0.2335	0.3345
375	0.0302	0.0412	0.0546	0.1031	0.1935	0.2839
400	0.0217	0.0316	0.0438	0.0878	0.1697	0.2516
425	0.0185	0.0280	0.0395	0.0814	0.1594	0.2374
450	0.0176	0.0257	0.0355	0.0714	0.1381	0.2048
475	0.0184	0.0250	0.0330	0.0620	0.1160	0.1700
500	0.0280	0.0332	0.0396	0.0627	0.1056	0.1486
525	0.0504	0.0545	0.0596	0.0779	0.1120	0.1461
550	0.0640	0.0674	0.0715	0.0863	0.1139	0.1415
575	0.0931	0.0960	0.0995	0.1122	0.1359	0.1596
600	0.2408	0.2437	0.2471	0.2595	0.2826	0.3057
625	0.3174	0.3206	0.3245	0.3389	0.3655	0.3922
650	0.3559	0.3601	0.3652	0.3837	0.4181	0.4525
675	0.4372	0.4410	0.4457	0.4626	0.4942	0.5257
700	0.6513	0.6530	0.6550	0.6623	0.6760	0.6896

<sup>a</sup> Reproduced from Austin and Petzold (1986), with permission.

The table on the right provides a simplified summary:	Type	$K_d(440)$	Chl
	I	0.017	0.01
	...		
This classification was greatly simplified by Morel and Prieur in 1977 who only distinguished between two cases, since phytoplankton and the associated detritus (both particulate and dissolved) are generally the most important optically active constituents in offshore waters.	III	0.14	2.00
	1	0.20	>2.00
	...		
	9	1.0	>10.00

In this case, it is considered that the phytoplankton concentration makes it possible to calculate the concentration of any derivative product. This is not the case near the coast or off river plumes where sediments and dissolved substances of non-local origin may independently affect the optical properties. These two situations are distinguished as Case 1 and Case 2 waters:

EAUX DU CAS I		EAUX DU CAS II
1. Phytoplancton <i>en concentration variable</i>		5. Séiments remis en suspension depuis le fond (près des côtes ou dans les zones peu profondes)
2. Débris associés <i>issus du broutage du zooplancton et de dégradation naturelle</i>		6. Particules terrigènes provenant des rivières ou des glaciers
3. Matière organique dissoute <i>libérée par le phytoplancton et ses débris</i>		7. Matière organique dissoute produite par érosions et lessivages des sols
4. Poussières éoliennes <i>transportées depuis les déserts par l'atmosphère</i>		8. Apports anthropogéniques

Table 1-1. D'après Gordon et Morel (1983). Classification des principaux constituants optiquement actifs, en fonction de leur présence dans les eaux du cas I et du cas II. Les poussières éoliennes ne font théoriquement pas partie des eaux du cas I. Leur présence, épisodique, est une source d'anomalie des modèles bio-optiques habituels aux eaux du cas I.

(courtesy P. Gernez)

### 3) Models for Kd and R

Different analytical formulations of Kd exist.

Gordon (1989b) modelled Kd using:  $Kd = \frac{a(\lambda) + b_b(\lambda)}{\cos(\theta_{sw})}$  Generally,  $a > b_b$ , hence Kd can be considered as the ratio  $\frac{a(\lambda)}{\cos(\theta_{sw})}$ .

$\theta_{sw}$  is the nadir angle of the transmitted ray in water with respect to the solar zenith angle in air (thus equal to  $\arcsin(\sin(\theta_s)/nw)$  with  $\theta_s$  the solar zenith angle in air and nw the index of refraction of water). Do(sky) is due to radiance from the sky.

Morel (1988) also worked on Kpar and proposed a formulation that depended on the chlorophyll concentration (see the corresponding articles on the website of the LOV, Laboratoire de Villefranche sur mer) to obtain a depth averaged Kpar for the entire euphotic

layer

$$K_{PAR}^- = 0.121 Chl^{0.428}$$

This formulation differs from the approach by Riley (1956) by 0.02 for Chl-a concentrations above 1mg/m<sup>3</sup>. It also differs at the origin since Riley used:

$$K = 0.04 + 0.0088 Chl + + 0.054 Chl^{2/3}$$

If we assume that  $R(z=0)$  be directly proportional to the backscattering  $b_b$  and inversely proportional to the absorption  $a$ , several studies (e.g., Gordon, 1975; Morel et Prieur, 1977) focused on obtaining a relation that linked these parameters. The most cited equation from these efforts is:

$$R(0) = f^* b_b/a \text{ often with } R(0) = 0.33 b_b/a.$$

However, there are much more complicated versions of this equation (e.g., Zaneveld, 1982, 1994; and summarized for Rrs in Werdell et al., 2013).

Non-exhaustive bibliography:

Zaneveld, J.R.V., 1982. Remotely sensed *reflectance* and its dependence on vertical structure: a theoretical derivation. *Applied Optics*, 21, 4146–4150

Howard R. Gordon, 1989a, *Can the Lambert-Beer-law be applied to the diffuse attenuation coefficient of ocean water ? Limnol.*

Howard R. Gordon, 1989b, *Dependence of the diffuse reflectance of natural waters on the sun angle.* Limnol.

### Modelling light in the sea from IOPs

After the atospheric correction, and based on combining the following definitions (omitting any spectral and angular dependencies):

$$R = \frac{E_u(-0)}{E_d(-0)} = f \frac{b_b}{a} \text{ and } Q = \frac{E_u(-0)}{L_u(-0)} \text{ and } L_w = L_u(-0) \frac{1 - \rho_F}{n^2}$$

and

$$E_d(0^-) = E_d(0^+) \frac{1 - \bar{\rho}}{1 - \bar{r}R}$$

with

$\rho_F(\theta, \lambda)$  Coefficient de réflexion interne (Fresnel) de la surface océanique, pour la longueur d'onde  $\lambda$ , et l'incidence  $\theta$

$\bar{\rho}$  Moyenne du coefficient de réflexion pour la surface océanique, pour tous les angles (environ 0,06)

$\bar{r}$  Réflexion moyenne à l'interface air-mer pour l'éclairement ascendant

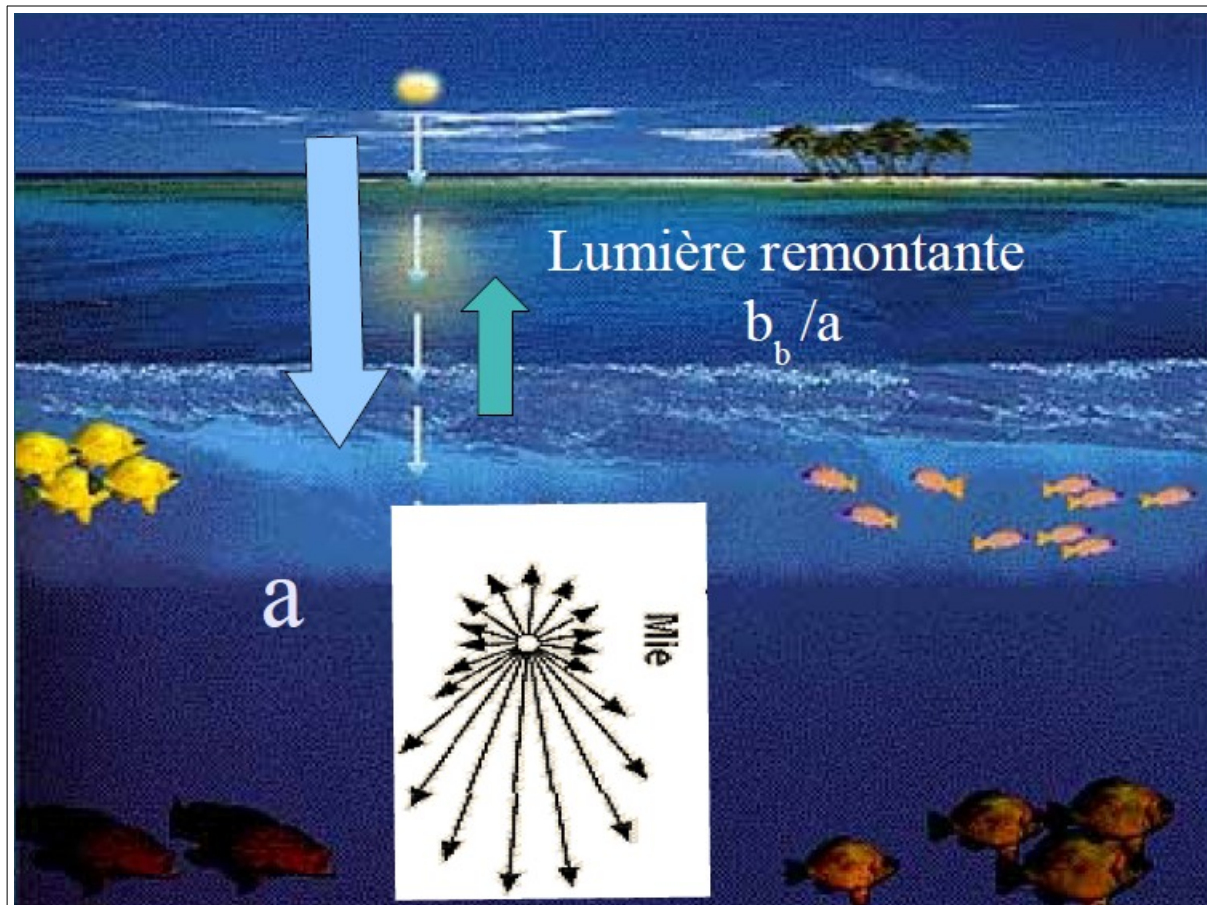
the marine radiance can be expressed as

$$L_w(\lambda, \theta_s, \theta', \Delta\phi) = E_d(0^+) \mathfrak{R}(\theta') \frac{f(\lambda, \theta_s)}{Q(\lambda, \theta_s, \theta', \Delta\phi)} \left[ \frac{b_b(\lambda)}{a(\lambda)} \right]$$

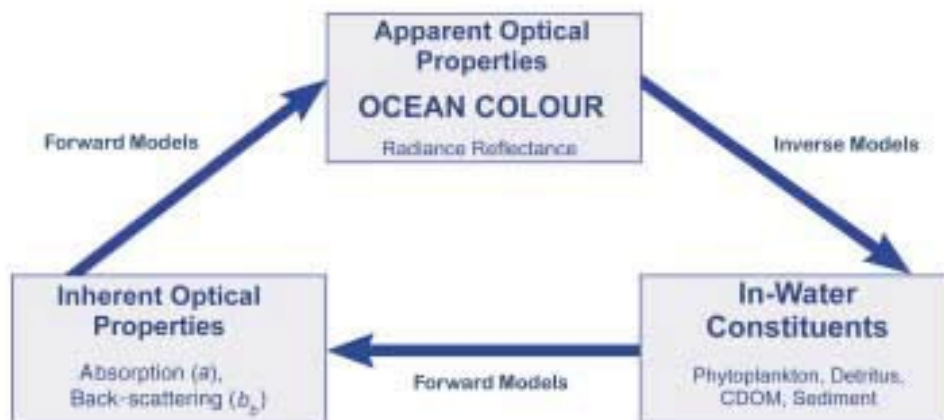
with  $\theta_s$  the solar zenith angle and

$\mathfrak{R}(\theta)$  Facteur rendant compte des effets de réflexion et de réfraction à la surface océanique  $\mathfrak{R}(\theta) = \left[ \frac{(1-\bar{\rho})}{(1-\bar{r}R)} \frac{(1-\rho_F(\theta))}{n^2} \right]$

What seems striking here is the anisotropy of these radiances, namely the fact that  $L_u$ , and especially  $L_w$ , differ for different viewing angles. This anisotropy depends on the shape of the volume scattering function (VSF), and also on the  $b/c$  and  $bw/b$  ratios. The anisotropy is described by the factor  $Q$ , the values of which were first theoretically deduced by Morel & Gentili (1993, 1996) before being verified experimentally (Morel et al., 1995).



## Summary of modelling using IOPs and AOPs:



(courtesy S. Alvain)

Difficulty in inverse modelling (i.e., doubt about the uniqueness of the solution):



Figure 1.2 (a) The direct problem: Describe the tracks of a dragon.

(b) The inverse problem: Describe a dragon from its tracks (from Bohren and Huffman, 1983.)

e.g., deriving IOPs from AOPs:

- 1) Loisel, H., Stramski, D., Dessailly, D., Jamet, C., Li, L., & Reynolds, R. A. (2018). *An Inverse Model for Estimating the Optical Absorption and Backscattering Coefficients of Seawater From Remote-Sensing Reflectance Over a Broad Range of Oceanic and Coastal Marine Environments.*, Journal of Geophysical Research: Oceans 123(3).

We present an inverse model (referred to as LS2) for estimating the inherent optical properties (IOPs) of seawater, specifically the spectral absorption,  $a(\lambda)$ , and backscattering,  $bb(\lambda)$ , coefficients within the ocean surface layer, from measurements of ocean remote-sensing reflectance,  $Rrs(\lambda)$ . The non-water absorption,  $anw(\lambda)$ , and particulate backscattering,  $bbp(\lambda)$ ,

coefficients can be derived after subtracting pure seawater contributions. The LS2 requires no spectral assumptions about IOPs and provides solutions at arbitrary light wavelengths in the visible spectrum independently of one another. As the LS2 can operate with the inputs of  $Rrs(\lambda)$  and solar zenith angle it is applicable to satellite ocean color remote sensing. The model can also operate with additional input of the diffuse attenuation coefficient of downward irradiance, which provides somewhat improved model performance for applications using in situ radiometric measurements as inputs. The evaluation of LS2 with a synthetic dataset that is free of measurement errors indicates good performance for IOPs in the visible spectrum, except for  $anw(\lambda)$  in the long-wavelength portion of the spectrum where  $anw(\lambda)$  contributes only a few percent to  $a(\lambda)$  under typical open ocean conditions. The good performance is characterized by a median absolute percentage difference between the model-derived and true values of IOPs, which is generally <20%, and the median ratio of model-derived to true values <10%. The satisfactory model performance is also demonstrated through validation analysis based on extensive datasets comprising coincident in situ measurements of  $Rrs(\lambda)$  and IOPs as well as a match-up dataset comprising satellite-derived  $Rrs(\lambda)$  and in situ IOP measurements. »

2) Werdell PJ, Jeremy, Franz BA, Bailey SW, Feldman GC, Boss E, Brando VE, Dowell M, Hirata T, Lavender SJ, Lee Z, Loisel H, Maritorena S, Mélin F, Moore TS, Smyth TJ, Antoine D, Devred E, d'Andon OH, Mangin A.

*Generalized ocean color inversion model for retrieving marine inherent optical properties.*

Appl Opt. 2013 Apr 1;52(10):2019-37. doi: 10.1364/AO.52.002019.

Ocean color measured from satellites provides daily, global estimates of marine inherent optical properties (IOPs). Semi-analytical algorithms (SAAs) provide one mechanism for inverting the color of the water observed by the satellite into IOPs. While numerous SAAs exist, most are similarly constructed and few are appropriately parameterized for all water masses for all seasons. To initiate community-wide discussion of these limitations, NASA organized two workshops that deconstructed SAAs to identify similarities and uniqueness and to progress toward consensus on a unified SAA. This effort resulted in the development of the generalized IOP (GIOP) model software that allows for the construction of different SAAs at runtime by selection from an assortment of model parameterizations. As such, GIOP permits isolation and evaluation of specific modeling assumptions, construction of SAAs, development of regionally tuned SAAs, and execution of ensemble inversion modeling. Working groups associated with the workshops proposed a preliminary default configuration for GIOP (GIOP-DC), with alternative model parameterizations and features defined for subsequent evaluation. In this paper, we: (1) describe the theoretical basis of GIOP; (2) present GIOP-DC and verify its comparable performance to other popular SAAs using both in situ and synthetic data sets; and, (3) quantify the sensitivities of their output to their parameterization. We use the latter to develop a hierarchical sensitivity of SAAs to various model parameterizations, to identify components of SAAs that merit focus in future research, and to provide material for discussion on algorithm uncertainties and future ensemble applications.

3) Roesler, C.S., and E. Boss. 2003. Ocean color inversion yields estimates of the spectral beam attenuation coefficient while removing constraints on particle backscattering spectra. *Geophysical Research Letters*, 30(9):1468

which is a non-dimensional form of  $c_p(\lambda) - a_p(\lambda)$ . In Roesler and Boss (2003), the basis vectors  $\mathbf{a}_{\text{phi}}$  and  $\mathbf{a}_{\text{NAP1}}$  were specified as in Roesler and Perry (1995) and the basis vector for beam attenuation was taken as

$$c_{p1} = \left( \frac{\lambda}{\lambda_0} \right)^{-\gamma}. \quad (8.21)$$

This latter assumption is based on the observations that variations in the functional form of the spectral dependence for  $c(\lambda)$  are more restricted than for  $b_{b,p}(\lambda)$ , and that spectral variations in  $b_{b,p}$  are weak. An interesting feature of this model is that inversion for IOPs produces not only the more standard  $a(\lambda)$  and  $b_b(\lambda)$  retrievals, but also  $c(\lambda)$  estimates.

Roesler and Boss (2003) applied this 'c-model' to invert measured  $R(\lambda)$  for IOPs, with  $\gamma$  and five amplitude terms derived by least-squares minimization. They also compared results to those for the standard Roesler and Perry (1995) model in which the basis vectors for particle backscattering are taken to follow simple power laws, that is as in (8.6). From this analysis, it was evident that both models can reproduce the major features of measured  $R(\lambda)$  for different water types, although the c-model performed better for fine details (Figures 8.18A, 8.18B). The c-model markedly outperformed the standard model in IOP retrieval (Figures 8.18C to 8.18H). Because inversion of the c-model provides estimates of  $c(\lambda)$  amplitude and spectral slope ( $\gamma$ ), there is potential for obtaining information about the shape of the particle size distribution (see Section 8.3.5 and Boss et al., 2001a, for example). Further assessment of this and related models, especially comparison of retrieval results with independent measurements for a variety of water types, is currently needed.

(Extract from "Real-time Coastal Observing Systems for Marine Ecosystem Dynamics and Harmful Algal Blooms: Theory, Instrumentation and Modelling", by Babin, Marcel, Roesler, Collin S., Cullen, John J., ed. Unesco, 2008)

Other reference for this extract:

Roesler, C. S., & Perry, M. J. (1995). In situ phytoplankton absorption, fluorescence emission, and particulate backscattering spectra determined from reflectance. *Journal of Geophysical Research*, 100, 13279–13294.